



EFFECT OF FLOW VELOCITY AND PARTICLE SIZE ON EROSION IN A PIPE WITH SUDDEN CONTRACTION

H.M. Badr¹, M.A. Habib¹, R. Ben-Mansour², and S.A.M. Said¹

1: Professor, Mechanical Engineering Department, KFUPM, Dhahran 31261

2: Assistant Professor, Mechanical Engineering Department, KFUPM, Dhahran 31261

ABSTRACT

Erosion is one of the important problems in various gas and liquid flow passages such as flow in pipes, pumps, turbines, compressors and many others. This paper deals with erosion prediction in a pipe with sudden contraction for the special case of two-phase (liquid and solid) turbulent flow with low sand particle concentration. The mathematical models for the calculations of the fluid velocity field and the motion of the solid particles have been established and an erosion model was used to predict the erosion rate. The fluid velocity (continuous phase) model is based on the time-averaged governing equations of axisymmetric turbulent flow while the particle-tracking model (discrete phase) is based on the solution of the governing equation of each particle motion taking into consideration the effect of particle rebound behavior. The solid particle concentration is assumed very small (volume ratio $< 10^{-3}$) such that the particles are not interacting within the flow field. It is also assumed that the solid particles motion has negligible effect on the fluid velocity. The effects of flow velocity and particle size were investigated considering water flow in a carbon-steel pipe with a sudden contraction of diameter ratio of 2:1. The results show the strong dependence of erosion on both flow velocity and particle size. The results also indicate the presence of a flow threshold velocity below which the erosion rate is negligibly small.

Keywords: erosion prediction, two phase flow particle-tracking.

1. INTRODUCTION

Erosion is one of the serious problems in various flow processes such as flow in pipes, pumps, turbines, compressors and many others. Accurate prediction of erosion requires detailed investigation of the solid particle motion before and after impact. Most flows occurring in industrial processes are turbulent which makes the particle trajectory and impact characteristics difficult to predict taking into consideration all fluid forces acting on the particle.

Erosion research can be classified under three categories; experimental investigations, erosion model developments, and numerical simulations. Most of the experimental studies determine the rate of erosion in pipes and pipe fittings and its relation with the other parameters involved in the process. Among these studies are the works by Roco et al. (1984), Venkatesh (1986), and Shook et al. (1987). The recent experimental study by McLaury et al. (1997) on erosion inside elbows and straight pipes provided correlations between the penetration rate and the flow velocity at different values of the elbow diameter and sand rate and size. Edwards et al. (2000) reported the effect of the bend angle on the normalized penetration rate. The objective of most of these studies was to provide data for establishing a relationship between the amount of erosion and the physical characteristics of the materials involved, as well as the particle velocity and angle of impact. Blanchard et al. (1984) carried out an experimental study of erosion in an elbow by solid particles entrained in water.

A number of erosion models/correlations were developed to provide a quick answer to design engineers in the absence of a comprehensive practical approach to be used for erosion prediction. One of the early erosion prediction correlations is that developed by Finnie (1958) expressing the rate of erosion in terms of particle mass and impact velocity. Nesic (1991) found that Finnie's model overpredicts the erosion rate and presented another formula in terms of a critical velocity rather than the impact velocity. Other erosion models were suggested by Salama and Venkatesh (1983), McLaury (1993) and Jordan (1998). Recently, Shirazi and McLaury (2000) presented a model for predicting multiphase erosion in elbows. An important different feature of this model was the use of the characteristic impact velocity of the particles.

The use of computational methods in erosion prediction constitutes a combination of flow modeling, Lagrangian particle tracking, and the use of erosion correlations. This approach is called the Lagrangian approach. Lagrangian models were developed by many researchers such as Wang et al. (1996), Keating and Nesic (2000) and Wallace et al. (2000). Wang et al. (1996) developed a computational model for predicting the rate of erosive wear in a 90° elbow for the two cases of sand in air and sand in water.

To the best of the authors' knowledge, most of the published work on erosion in pipes focused on straight pipes and pipe fittings such as bends and elbows. The erosion process occurring in a pipe with sudden contraction or sudden enlargement was not considered in any previous

study. The present research work aims at studying the effects of flow velocity and particle size on erosion in a pipe contraction under conditions simulating the actual working conditions.

2. PROBLEM STATEMENT AND METHOD OF SOLUTION

The problem considered is that of erosion in a large pipe of diameter, $D=200$ mm, connected to a small pipe of diameter, d , as shown in Figure 1 with diameter ratio 2:1. The pipe centerline is always vertical while the direction of fluid flow is either upward or downward. Both pipes are made of carbon steel and the length of each pipe is chosen in such a way to justify the assumption of fully developed flow at the entrance and exit sections of the flow domain. The fluid considered is water at 20°C with low particle concentration such that the effect of particle motion on the fluid flow field is negligibly small. The main parameters affecting the erosion in the up-flow and down-flow configurations are the flow velocity and particle size and concentration. The Lagrangian particle tracking method is used to model the erosion process and is normally carried out utilizing the following steps [Wallace et al. (2000)]:

- a) Predict the flow velocity field in the domain of interest.
- b) Calculate the trajectories of solid particles entrained in the fluid using Lagrangian particle tracking calculations and then extract the particle impact data.
- c) Predict the erosive wear using semi-empirical equations.

The approach represents a one-way flow-to-particle coupling method that can be used when low volume of particles is simulated. Two computational models were developed. The first is the continuous phase model (dealing with the prediction of the flow velocity field) and the second is the particle-tracking model (dealing with the prediction of particle motion). A brief discussion of the two models is presented in the following sections.

2.1 THE CONTINUOUS PHASE MODEL

A combination of computational fluid dynamics and Lagrangian particle tracking are normally used to predict the particle movement through complex geometries. To predict the flow pattern of the continuous flow phase, the conservation equations for mass and momentum are solved together with the transport equations for the turbulence model. The time-averaged governing equations of axisymmetric turbulent flow can be found in many references [Habib et al. (1989) and Versteeg and Malalasekera (1995)] and can be presented as follows.

$$\frac{\partial}{\partial x_j}(\rho \bar{U}_j) = 0 \quad (1)$$

$$\frac{\partial}{\partial x_j} \left(\rho \overline{U_i U_j} \right) = -\frac{\partial p}{\partial x_i} + \frac{\partial}{\partial x_j} \left(\mu \frac{\partial U_i}{\partial x_j} \right) - \frac{\partial}{\partial x_j} \left(\rho \overline{u_i u_j} \right) \quad (2)$$

where p is the static pressure and the stress tensor $\overline{\rho u_i u_j}$ is given by

$$-\rho \overline{u_i u_j} = \left[\mu_t \left(\frac{\partial \overline{U_i}}{\partial x_j} + \frac{\partial \overline{U_j}}{\partial x_i} \right) \right] - \frac{2}{3} \rho k \delta_{ij} \quad (3)$$

where δ_{ij} is the Kronecker delta and $\mu_{eff} = \mu_t + \mu$ is the effective viscosity. The turbulent viscosity, μ_t , is calculated using the high-Reynolds number form as

$$\mu_t = \rho C_\mu \frac{k^2}{\varepsilon} \quad (4)$$

with $C_\mu = 0.0845$ [Reynolds 1987], k and ε are the kinetic energy of turbulence and its dissipation rate. These are obtained by solving the following conservation equations [Reynolds (1987) and Shih et al. (1995)]:

$$\frac{\partial}{\partial x_j} (\rho \overline{U_j k}) = \frac{\partial}{\partial x_j} \left(\frac{\mu_{eff}}{\sigma_k} \frac{\partial k}{\partial x_i} \right) + G_k - \rho \varepsilon \quad (5)$$

$$\frac{\partial}{\partial x_j} (\rho \overline{U_j \varepsilon}) = \frac{\partial}{\partial x_i} \left(\frac{\mu_{eff}}{\sigma_\varepsilon} \frac{\partial \varepsilon}{\partial x_i} \right) + C_1 G_k \frac{\varepsilon}{k} - C_2^* \rho \frac{\varepsilon^2}{k} \quad (6)$$

where G_k represents the generation of turbulent kinetic energy due to the mean velocity gradients and is given by

$$G_k = -\rho \overline{u_i u_j} \frac{\partial \overline{U_j}}{\partial x_i} \quad (7)$$

The quantities σ_k and σ_ε are the effective Prandtl numbers for k and ε , respectively and C_2^* is given by Shih et al. (1995) as

$$C_2^* = C_2 + C_3 \quad (8)$$

where C_3 is a function of the term k/ε and, therefore, the model is responsive to the effects of rapid strain and streamline curvature and is suitable for the present calculations. The model constants C_1 and C_2 have the values; $C_1=1.42$ and $C_2=1.68$. The wall functions establish the link between the field variables at the near-wall cells and the corresponding quantities at the wall. These are based on the assumptions introduced by Launder and Spalding (1974) and have been most widely used for industrial flow modeling. The details of the wall functions are provided by the law-of-the-wall for the mean velocity as given by Habib et al. (1989).

The velocity distribution is considered fully developed at the inlet section. The kinetic energy of turbulence is assigned the value $k = 0.01\bar{U}^2$ while the dissipation rate of turbulent kinetic energy is specified using equation (4) with μ_t expressed in terms of a length scale L , where L was taken equal to the inlet pipe diameter. The boundary condition applied at the exit section is that of fully developed pipe flow. At the wall boundaries, all velocity components are set to zero in accordance with the no-slip and impermeability conditions. Kinetic energy of turbulence and its dissipation rate are determined from the equations of the law of the wall.

The conservation equations are integrated over a typical volume that is formed by division of the flow field into a number of control volumes, to yield the solution. The equations are solved simultaneously using the solution procedure described by Patankar (1980). Calculations are performed with at least 300,000 control volumes considering small volumes in the vicinity of the contraction section where the variations of flow properties are expected to be large. This large number of control volumes ensures grid independent results. Convergence is considered when the maximum of the summation of the residuals of all the elements for U , V , W and pressure correction equations is less than 0.1 %.

2.2 PARTICLE TRACKING

The particle tracking calculations aim to determine the particle trajectory as well as its velocity (magnitude and direction) before every impact either on the pipes walls or anywhere on the tube sheet. Such impact velocity is not only important for the calculation of solid surface erosion but also important in the determination of the particle trajectory during its subsequent course of motion following impact. In this work, the solid particles are assumed not to interact with each other and the influence of particle motion on the fluid flow field is assumed very small and can be neglected. These two assumptions are based on the condition of fairly dilute particle concentration. The same assumptions were made by many researchers such as Lu et al. (1993), Shirazi et al. (1995), Edwards et al. (2000), and Wallace et al. (2000) in the solution of similar problems of low particle concentration (less than 2–3% by weight). Taking the main hydrodynamic forces into consideration, the particle equation of motion can be written as:

$$\frac{d\mathbf{u}_p}{dt} = F_D(\mathbf{u} - \mathbf{u}_p) + \mathbf{g}(\rho_p - \rho)/\rho_p + \mathbf{F}_{vm} + \mathbf{F}_{pg} + \mathbf{F}_{sl} \quad (9)$$

where $F_D(\mathbf{u} - \mathbf{u}_p)$ is the drag force per unit particle mass and $F_D = 3C_D\mu R_{ep}/4\rho_p D_p^2$, $\mathbf{g}(\rho_p - \rho)/\rho_p$ is the buoyancy force term, \mathbf{F}_{vm} is the virtual mass term (force required to accelerate the fluid surrounding the particle), \mathbf{F}_{pg} is the pressure gradient term and \mathbf{F}_{sl} is the Saffman lift force [Saffman (1965)]. The Magnus lift force (resulting from particle rotation) and the Basset history force (the force accounting for the flow field unsteadiness) have been neglected. The particle Reynolds number, R_{ep} , and the drag coefficient, C_D , are obtained from

$$R_{ep} = \frac{\rho D_p |u_p - u|}{\mu} \tag{10}$$

$$C_D = a_1 + \frac{a_2}{R_{ep}} + \frac{a_3}{R_{ep}^2} \tag{11}$$

where the a 's are constants given by Morsi and Alexander (1972) for smooth spherical particles over several ranges of Re . Another equation that is frequently used for C_D [Haider and Levenspiel (1989)] is given by

$$C_D = \frac{24}{R_{ep}} (1 + b_1 R_{ep}^{b_2}) + \frac{b_3 R_{ep}}{b_4 + R_{ep}} \tag{12}$$

where b_1, b_2, b_3 and b_4 are constants that depend on the volume and surface area of the solid particles.

In the present study, the dominant forces are the drag and buoyancy forces since the other forces given in equation (9) are of small order of magnitude and can be neglected. The particle velocity, u_p , is first obtained by stepwise integration of the particle equation of motion (9) over a discrete time step. The particle trajectory is then predicted by integrating the simple equation

$$\frac{dr}{dt} = u_p, \tag{13}$$

where r is the position vector. The above equation is integrated in each coordinate direction to predict the trajectories of the discrete phase. During the integration, the fluid phase velocity, u , is taken as the velocity of the continuous phase at the particle position.

The boundary conditions considered when a particle strikes a boundary surface depends on the nature of that surface and it can be a reflection via an elastic or inelastic collision [Tabakoff and Wakeman (1982)] or escape through an open boundary. The trajectory calculations for some particles (normally very few) are terminated when the particles get trapped in the flow field. This is found to occur when a particle circulates in a confined flow zone.

2.3 THE EROSION MODEL

Erosion is defined as the wear that occurs when solid particles entrained in a fluid stream strike a surface. The previous experimental results [Davies et al. (1991) and Isomoto, et al. (1999)] show that the erosive wear-rate exhibits a power-law velocity dependence. The velocity exponent ranges from 1.9 to 2.5. The results also indicate that erosion depends on the angle of impact. The influence of the impact angle depends greatly on the type of material being brittle or ductile. Prediction of erosion in straight pipes, elbows and tees show the strong influence of fluid properties, sand size and flow velocity on the rate of erosion [Postletwaite and Nesic (1993) and McLaury and Shirazi (1998)]. The complexity of the erosion process and the number of factors involved made it difficult for obtaining an analytical formula that could be used to predict erosion under any condition. Almost all of the formulae generated have therefore some degree of dependence on empirical coefficients provided by various experimental erosion tests. No definitive theory of erosion currently exists, however, a number of qualitative and quantitative models do exist. These were described by Finnie (1958) and Finnie et al (1992), Wang et al (1996), Keating and Nesic (2000), Edwards et al (2000) and Shirazi and McLaury (2000).

The empirical erosion equations suggested by Neilson and Gilchrist (1968) were later used by Wallace et al. (2000) to correlate the experimental erosion data in order to develop an erosion modeling technique. Wallace et al. (2000) provided the following formulae that resulted in good accuracy when compared to previous experimental data:

$$E = \left\{ \frac{\frac{1}{2}u_p^2 \cos^2 \alpha \sin 2\alpha}{\gamma} + \frac{\frac{1}{2}u_p^2 \sin^2 \alpha}{\sigma} \right\} \text{ for } \alpha \leq 45^\circ \quad (14a)$$

$$E = \left\{ \frac{\frac{1}{2}u_p^2 \cos^2 \alpha}{\gamma} + \frac{\frac{1}{2}u_p^2 \sin^2 \alpha}{\sigma} \right\} \text{ for } \alpha > 45^\circ \quad (14b)$$

where γ and σ are the cutting wear and deformation wear coefficients having the values 33316.9 and 77419.7 respectively. In the present study, equations (14a,b) are used for calculating the erosion rate.

Using the particle-tracking model, the impingement data (impact speed and angle) were first compiled for all particles impacting the solid boundaries of the flow domain. The compiled data were then used together with the erosion model (14a,b) for computing the erosion rate at different locations on the tube sheet. The erosion rate calculations were performed using equations (14a,b) via a FORTRAN subroutine that was linked to the CFD code.

3. RESULTS AND DISCUSSION

The above-described model was used to calculate the rate of erosion in a pipe with sudden contraction for the two cases of upflow and downflow when the contraction ratio, $d/D = 0.5$ as shown in Figure 1. The upstream pipe diameter is 200 mm and the considered average velocities of the approaching flow were 1 m/s, 5 m/s and 10 m/s. The fluid considered is water at 20°C ($\rho = 998 \text{ kg/m}^3$ and $\mu = 1 \text{ mPa}\cdot\text{s}$) which results in flow Reynolds number (based on the diameter of the large pipe, D) ranging from 2×10^5 to 2×10^6 . The solid particles are considered sand particles of spherical shape with diameters 10 μm , 100 μm , 200 μm and 400 μm .

A number of investigations were first carried out in order to determine the critical erosion areas in the flow domain. These investigations covered the entire ranges of flow velocity and particle diameter. It was found that erosion occurs mainly in the contraction plate ABCD (which will be referred to as the tube sheet) shown in Figure 1 while being insignificant elsewhere. Figure 2 shows the trajectories of a number of particles released at the same time at the inlet section of the flow field when the flow velocity is 10 m/s and the particle diameter is 400 μm . The figure shows that almost all particle impacts occur on the flat surface ABCD while impacts on the pipe walls are insignificant. Accordingly, erosion data will be presented only at section ABCD.

The variation of the local erosion rate on the tube sheet is shown in Figure 3 for the case of upflow. This tube sheet has the shape of an annulus with inner radius, $r/R = 0.5$, and outer radius, $r/R = 1.0$, where $R = D/2$. The erosion rates are obtained for each of the four particle sizes at each value of the inflow velocity as shown in Figures 3a-d. The results indicate that for particles of small diameter ($D_p = 10 \mu\text{m}$), the erosion rate is negligibly small in the outer region of the annular plate ($0.67 \leq r/R \leq 1.0$) and reaches its maximum close to the entrance of the small pipe ($r/R \approx 0.5$) as shown in Figure 3a. The highest rate of erosion ($E \approx 1.6 \times 10^{-4} \text{ mg/g}$) was found when the velocity of flow is maximum (10 m/s) and decreases rapidly with the decrease of flow velocity until becoming negligibly small when the flow velocity reaches 1 m/s. Although the rate of erosion increases with the increase of particle diameter as shown in Figures 3b-d, the trend is almost the same in the four cases. However, for large particle size ($D_p = 400 \mu\text{m}$), the region of negligible erosion for all flow velocities diminishes to ($0.83 \leq r/R \leq 1.0$) which is much smaller than that obtained in the case of small particle sizes. The other interesting feature that is common in the four figures is the absence of erosion for all particle sizes in the entire flow domain in the case of low flow velocity (1 m/s). Qualitatively, such behavior is in conformity with the erosion prevention criterion established by API (1981) in which a threshold velocity was set by the recommended practice API RP 14E for eliminating erosion. Another criterion for the threshold velocity was developed by Salama and Venkatesh (1983) for erosion in elbows.

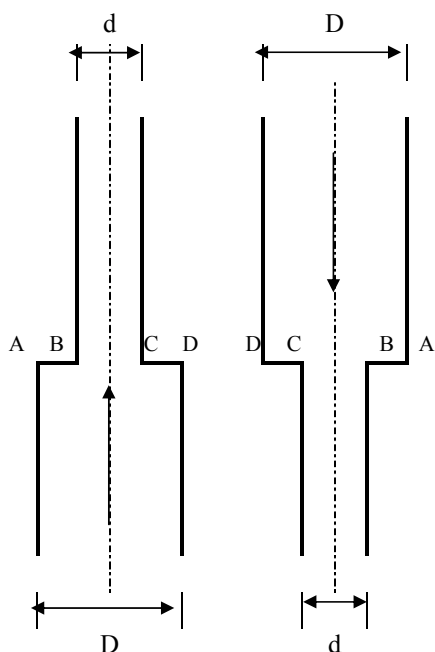


Figure 1. Flow passage geometry for the two cases of up-flow and down-flow.

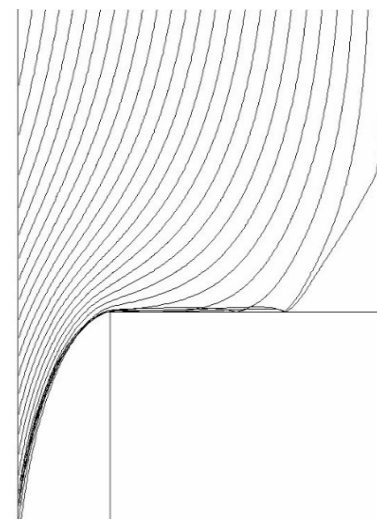


Figure 2. The trajectories of a number of particle released at the same time at the inlet section showing impact on the contraction plate for the case of downflow with $V_i=10\text{m/s}$ and $D_p=400\ \mu\text{m}$.

The variation of the local erosion rate presented in Figure 3 can be explained on the basis of the streamline pattern plotted in Figure 4a for the case when the flow velocity is 5 m/s. The figure shows a recirculating flow region upstream of the contraction section and extending to the tube sheet (ABCD). An enlarged view of that region is shown in Figure 4b. The flow velocity in this region is very small and the presence of solid particles, if any, in such low velocity zone will cause negligible erosion in accordance with equations (14a,b). The figure also shows that this recirculating flow zone occupies the area on the tube sheet between $r/R \approx 0.72$ and $r/R = 1.0$. This is approximately the same area characterized by negligible erosion in Figures 4a-d. Moreover, the maximum erosion rate occurs in a region where the approaching flow has high velocity and large curvature. Both effects will give rise to higher particle velocity that impacts the surface of the annular plate close to $r/R \approx 0.5$. These features are confirmed by the particle trajectories given in Figure 2 that clearly shows the high intensity of particle impact on the contraction plate in the region close to $r/R \approx 0.5$. The effect of flow velocity on the total rate of erosion occurring on the annular plate is presented in Figure 5 for the four different particle sizes. The strong dependence of erosion on flow velocity is very clear in the figure. From the obtained results, it is also clear that there is a threshold velocity, V_c , below which erosion is insignificant.

The erosion rates obtained for the downflow case are presented in Figure 6 for the same particle diameters and inlet flow velocities. The results are almost the same as those obtained

in the upflow case except in Figure 6d ($D_p=400\ \mu\text{m}$) that shows higher rate of erosion ($\approx 50\%$ increase) at a flow velocity of 5 m/s. It is quite expected that the effect of gravity on particle motion becomes significant at low flow velocities. However, such effect did not influence the rate of erosion at the lowest flow velocity (1 m/s) because such velocity is considerably below the threshold velocity, V_t . On the other hand, the flow velocity of 5 m/s is definitely above the threshold velocity (see Figure 6) and the effect of gravity becomes sensible. A quick comparison of the data presented in Figures 3 and 6 shows that the effect of gravity on the rate of erosion is very small in the case of high inlet flow velocity (10 m/s) for all particle sizes. This can be explained based on the fact that the relative contribution of gravity to the motion of solid particles gets smaller with the increase of flow velocity. Figure 7 shows the variation of the total erosion rate at the contraction section with flow velocity for different particle sizes. Although the trends are the same as in Figure 5 the values obtained are slightly different especially in the case of moderate flow velocity (5 m/s) and large particle size ($D_p=400\ \mu\text{m}$).

4. CONCLUDING REMARKS

The problem of erosion in a vertical pipe with sudden contraction was investigated for the special case of two-phase turbulent flow with low particle concentration. The flow was either in direction of gravity (downflow) or against it (upflow). The study focused on the effects of flow velocity and particle size and was limited to one contraction geometry and one fluid. Two mathematical models were used; one for the determination of the fluid velocity field and the other for the solid particle trajectory in addition to an erosion model that was used to predict the erosion rate. The flow velocity in the large pipe ranged from 1 m/s to 10 m/s and the particle size ranged from $10\ \mu\text{m}$ to $400\ \mu\text{m}$. In these ranges, the results showed the strong dependence of erosion on both particle size and flow velocity but with little dependence on the direction of flow. The effect of flow direction was found to be significant only for large particle size ($400\ \mu\text{m}$) and moderate flow velocity (5 m/s). The erosion critical area was found to be the inner surface of the tube sheet (connecting the two pipes) in the region close to the small pipe. The results also indicated the presence of a threshold velocity below which erosion is insignificant for all particle sizes.

ACKNOWLEDGMENTS

The authors wish to acknowledge the support received from King Fahd University of Petroleum & Minerals during this study.

NOMENCLATURE

b	constant defined in equation (12)
C_D	drag coefficient
C_μ	constant defined in equation (4)
C_1	constant defined in equation (6)
C_2	constant defined in equation (8)
C_2^*	constant defined in equation (6)
d	pipe diameter at exit
D	pipe diameter at inlet
D_p	Solid particle diameter
E	Erosion rate, mg/g
F	force
G_k	generation of turbulent kinetic energy
g	gravitational acceleration
k	turbulent kinetic energy
p	pressure
Re_p	particle Reynolds number
$\overline{U_j}$	average velocity component
\underline{u}	fluid velocity vector
u_j	fluctuating velocity component
u_p	particle velocity
V_i	Flow inlet velocity
V_t	Threshold “erosional” velocity
u_p	particle velocity
x_j	space coordinate
t	time

Greek letters

α	impact angle
ϵ	dissipation rate of turbulent kinetic energy
μ	dynamic viscosity
ρ	density
σ_k	effective Prandtl number for k
σ_ϵ	effective Prandtl number for ϵ

Superscripts

•	time rate
—	time average

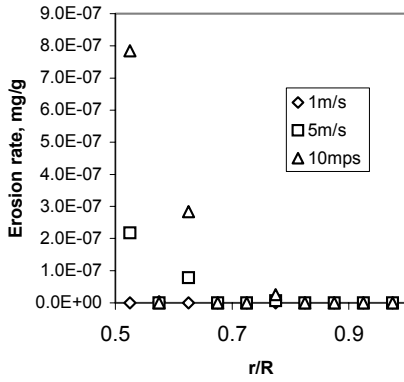
Subscripts

D	drag
f	fluid
sl	Saffman lift
lc	local
m	target material
p	particle
pg	pressure gradient
vm	virtual mass

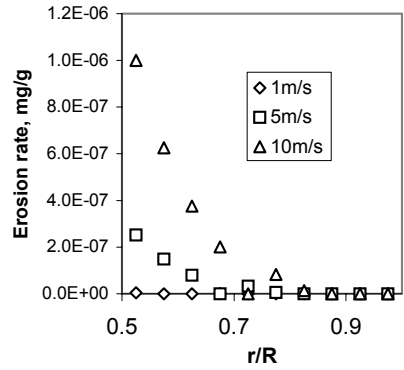
REFERENCES

1. API Recommended Practice for Design and Installation of Offshore Production Platform Piping Systems, API RP 14E (1981). American Petroleum Institute, Third Edition, Washington D.C., Dec. 1981.
2. Blanchard, D.J., P. Griffith and E. Rabinowicz (1984). Erosion of a pipe bend by solid particle entrained in water. *J. of Engineering for industry*, Vol. 106, pp. 213-217.
3. Davies, J.E., Stead, R.J., Andrews, C.J. and Richards, J.R. (1991). The airborne particle erosion resistance of a Range of engineering materials, *Key Engineering Materials*, Vol. 117, pp. 45-52.
4. Edwards J.K., B.S. McLaury and S.A. Shirazi (2000). Evaluation of alternative pipe bend fittings in erosive service. Proceedings of 2000 ASME Fluids Engineering Summer Meeting, June 11-15, 2000, Boston, MA, Paper No. FEDSM2000-11245.
5. Finnie, I. (1958). The mechanism of erosion of ductile metals, Proceedings of 3rd US National Congress of Applied Mechanics, pp. 527-532.
6. Finnie, I., G.R. Stevick and J.R. Ridgely (1992). The influence of impingement angle on the erosion of ductile metals by angular abrasive particles, *Wear*, Vol. 152, pp. 91-98.
7. Habib, M.A., A. E. Attya and D. M. McEligot (1989). Calculation of turbulent flow and heat transfer in channels with streamwise periodic flow, *ASME Journal of Turbomachinery*, Vol 110, pp. 405-411.
8. Haider, A. and O. Levenspiel (1989). Drag Coefficient and Terminal Velocity of Spherical and Nonspherical Particles, *Powder Technology*, Vol. 58, pp. 63-70.
9. Isomoto, Y., Nishimura, M., Nagahashi, K. and Matsumura, M (1999). Impact angle dependence of erosion by solid particle impact for metallic materials, *Erosion Engineering*, Vol. 48, No. 6, pp. 355-361.
10. Jordan, K. (1998). Erosion in multiphase production of oil and gas, Corrosion 98, paper n. 58, NACE International Annual Conference, San Antonio.
11. Keating, A. and S. Nestic (2000). Particle tracking and erosion prediction in three-dimensional bends, Proceedings of 2000 ASME Fluids Engineering Summer Meeting, June 11-15, 2000, Boston, MA, Paper No. FEDSM2000-11249.
12. Launder, B.E. and D. B. Spalding (1974). The numerical computation of turbulent flows, *Computer Methods in Applied Mechanics and Engineering*, Vol. 3, pp. 269-289.
13. Lu, Q.Q., J.R. Fontaine and G. Aubertin (1993). A Lagrangian model for solid particles in turbulent flows, *Int. J. Multiphase Flow*, Vol. 19, No. 2, pp. 347-367.
14. McLaury, B. S. and Shirazi, S. A (1998). Predicting Erosion in Straight Pipes, *Proceedings of the 1998 ASME Fluids Engineering Division, FEDSM 98-5226*, June 21-25, Washington D. C.
15. McLaury, B.S. (1993). A model to predict solid particle erosion in oil field geometries. M.S. Thesis, The University of Tulsa.
16. McLaury, B.S., J. Wang, S.A. Shirazi, J.R. Shadley and E.F. Rybicki (1997). Solid particle erosion in long radius elbows and straight pipes, Society of Petroleum Engineers, Paper No. SPE 38842, pp. 977-986.
17. Morsi, S.A. and A.J. Alexander (1972). An investigation of particle trajectories in two-phase flow systems. *Journal of Fluid Mechanics*, Vol. 52, No. 2, pp. 193-208.

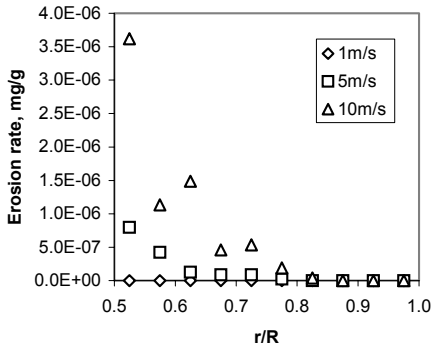
18. Neilson, J.H. and Gilchrist, A. (1968). Erosion by a stream of solid particles, *Wear*, Vol. 11, pp. 111-122.
19. Nestic, S. (1991). Computation of localized erosion-corrosion in disturbed two-phase flow, Ph.D. thesis, University of Saskatchewan, Saskatoon, Canada.
20. Patankar, S.V. (1980). *Numerical Heat Transfer and Fluid Flow*, First Edition, Taylor and Francis.
21. Postletwaite, J. and Nestic, S (1993). Erosion in Disturbed Liquid/ Particle Pipe Flow; Effects of Flow Geometry and Particle Surface Roughness, *Corrosion* v49 n10, Oct, PP850-859.
22. Reynolds, W.C. (1987). Fundamentals of turbulence for turbulence modeling and simulation, *Lecture Notes for Von Karman Institute*, Agard Report No. 755.
23. Roco, M. C., P. Nair, G.R. Addie and J. Dennis (1984). Erosion of Concentrated Slurries in Turbulent Flow. *Journal of Pipelines* Vol. 4, pp213-221.
24. Saffman, P.G. (1965). The lift on a small sphere in a slow shear flow. *Journal of Fluid Mechanics*, Vol. 22, No. 2, pp. 385-400.
25. Salama, M.M. and E.S. Venkatesh (1983). Evaluation of Erosional Velocity Limitations of Offshore Gas Wells, 15th Annual OTC, Houston, TX, May 2-5, OTC No. 4485.
26. Shih, T.H., W. W. Liou, A. Shabir, and J. Zhu (1995). A new k- ϵ eddy-viscosity model for high Reynolds number turbulent flows - Model development and validation, *Computers and Fluids*, Vol. 24, No. 3, pp. 227-238.
27. Shirazi, S. A., Shadley, J.R., McLaury, B.S., and Rybicki, E.F. (1995). A procedure to predict solid particle erosion in elbows and tees, *Journal of Pressure Vessel Technology*, Vol. 117, pp.45-52.
28. Shirazi, S.A., and McLaury, B.S. (2000). Erosion modeling of elbows in multiphase flow, Proceedings of 2000 ASME Fluids Engineering Summer Meeting, June 11-15, 2000, Boston, MA, Paper No. FEDSM2000-11251.
29. Shook, C. A., M. Mckibben and M. Small (1987). Experimental Investigation of Some Hydrodynamics Factors Affecting Slurry Pipeline Wall erosion, ASME Paper No. 87-PVP-9.
30. Tabakoff, W. and T. Wakeman (1982). Measured particle rebound characteristics useful for erosion prediction, ASME paper 82-GT-170.
31. Venkatesh, E. S. (1986). Erosion Damage in Oil and Gas Wells, SPE paper 15183, Rocky Mountain Regional Meeting, of the Society of Petroleum Engineers, Billings, MT.
32. Versteeg, H. K. and Malalasekera, W. (1995). *An Introduction to Computational Fluid Dynamics; The Finite Volume Method*, Longman Scientific and Technical, London.
33. Wallace, M.S., J.S. Peters, T.J. Scanlon, W.M. Dempster, S. McCulloch and J.B. Ogilvie (2000). CFD-based erosion modeling of multi-orifice choke valves, Proceedings of 2000 ASME Fluids Engineering Summer Meeting, June 11-15, 2000, Boston, MA, Paper No. FEDSM2000-11244.
34. Wang, J., S.A. Shirazi, J.R. Shadley and E.F. Rybicki (1996). Application of flow modeling and particle tracking to predict sand erosion rates in 90-degree elbows. FED-Vol. 236, 1996 ASME Fluids Engineering Division Conference, Vol. 1, pp. 725-734.



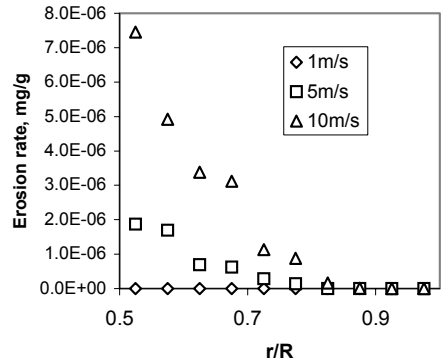
a) $D_p = 10 \mu\text{m}$



b) $D_p = 100 \mu\text{m}$



c) $D_p = 200 \mu\text{m}$



d) $D_p = 400 \mu\text{m}$

Figure 3. The radial variation of the local erosion rate on the contraction plate (ABCD) for the case of upflow: a) $D_p = 10 \mu\text{m}$, b) $D_p = 100 \mu\text{m}$, c) $D_p = 200 \mu\text{m}$, d) $D_p = 400 \mu\text{m}$.

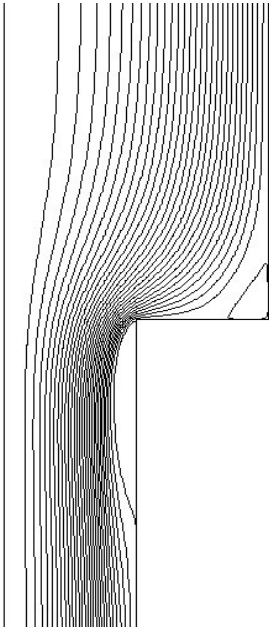


Figure 4a. The streamline pattern for the case of $V_i=5\text{m/s}$.

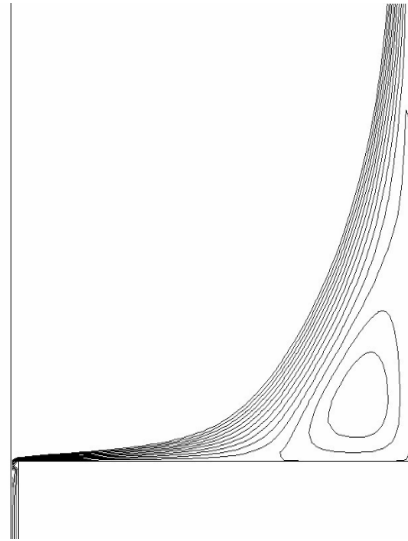


Figure 4b. An enlarged view of the circulatory flow zone at the contraction region – case of $V_i=5\text{m/s}$.

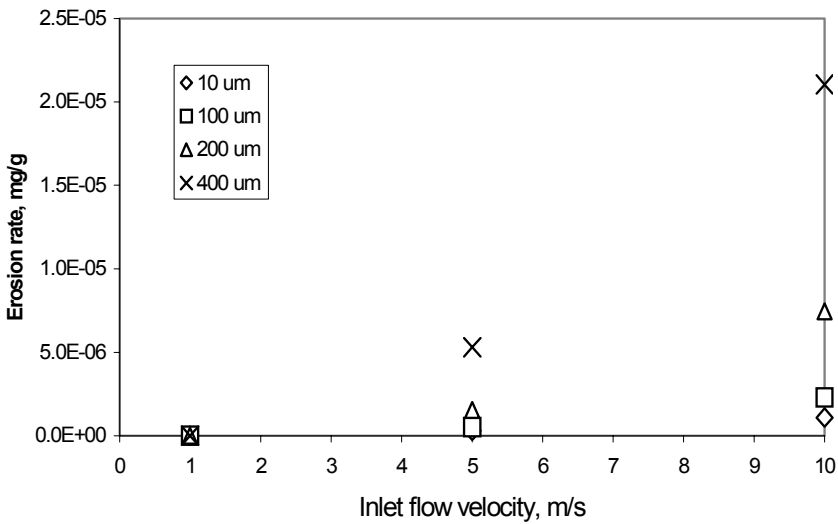
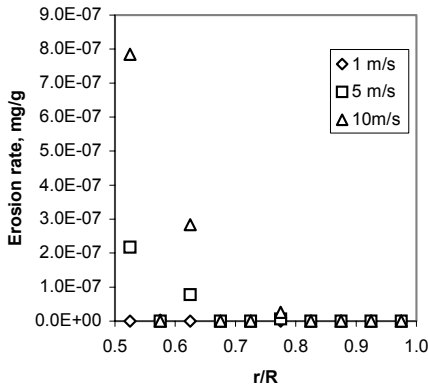
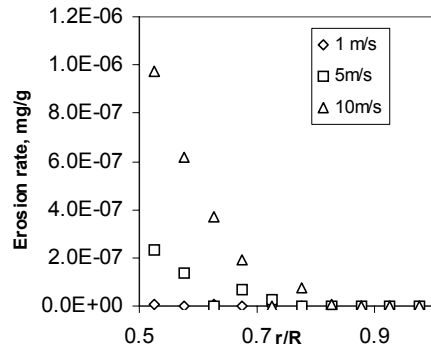


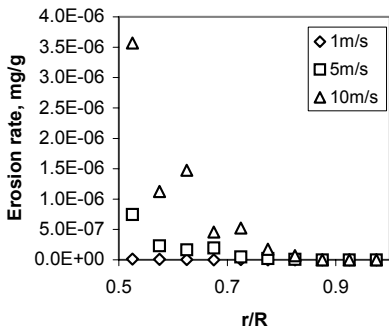
Figure 5. The effect of inlet flow velocity on the total rate of erosion occurring on the tube sheet for different particle diameters in the case of upflow.



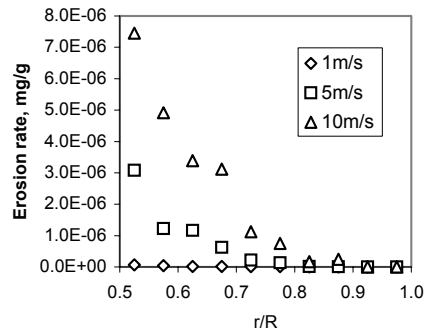
a) $D_p = 10 \mu\text{m}$



b) $D_p = 100 \mu\text{m}$



c) $D_p = 200 \mu\text{m}$



d) $D_p = 400 \mu\text{m}$

Figure 6. The radial variation of the local erosion rate on the contraction plate (ABCD) for the case of downflow: a) $D_p = 10 \mu\text{m}$, b) $D_p = 100 \mu\text{m}$, c) $D_p = 200 \mu\text{m}$, d) $D_p = 400 \mu\text{m}$.

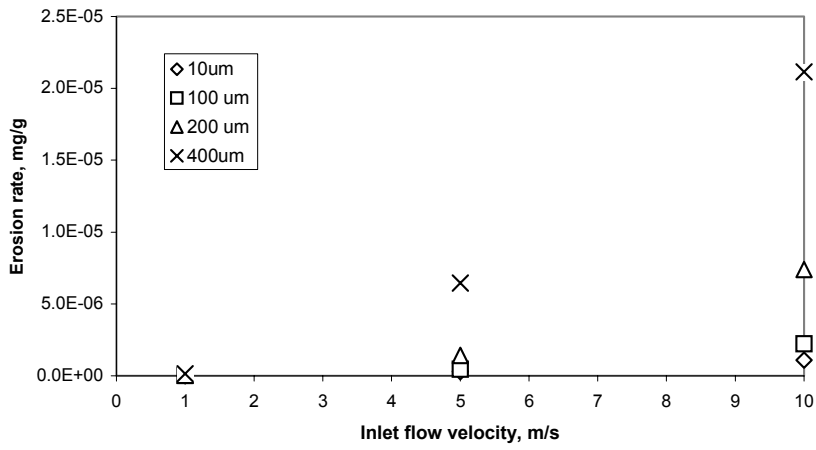


Figure 7. Effect of inlet flow velocity on the total rate of erosion occurring on the tube sheet for different particle diameters in the case of downflow.